

The Spin Glass Phase in the Four-State, Three-Dimensional Potts Model

A. Cruz,^{1,2} L.A. Fernandez,^{3,2} A. Gordillo-Guerrero,^{4,2} M. Guidetti,⁵ A. Maiorano,^{5,2} F. Mantovani,⁵ E. Marinari,⁶
V. Martin-Mayor,^{3,2} A. Muñoz Sudupe,³ D. Navarro,⁷ G. Parisi,⁶ S. Perez-Gaviro,² J. J. Ruiz-Lorenzo,^{8,2}
S.F. Schifano,⁵ D. Sciretti,^{1,2} A. Tarancon,^{1,2} R. Tripiccione,⁵ J.L. Velasco,² D. Yllanes,^{3,2} and A.P. Young⁹

¹*Departamento de Física Teórica, Universidad de Zaragoza, 50009 Zaragoza, Spain.*

²*Instituto de Biocomputación y Física de Sistemas Complejos (BIFI), Zaragoza, Spain.*

³*Departamento de Física Teórica I, Universidad Complutense, 28040 Madrid, Spain.*

⁴*Dpto. de Ingeniería Eléctrica, Electrónica y Automática, Universidad de Extremadura. Avda. de la Universidad s/n. 10071. Cáceres, Spain.*

⁵*Dipartimento di Fisica Università di Ferrara and INFN - Sezione di Ferrara, Ferrara, Italy.*

⁶*Dipartimento di Fisica, INFN and INFN, Università di Roma “La Sapienza”, 00185 Roma, Italy.*

⁷*Departamento de Ingeniería, Electrónica y Comunicaciones and Instituto de Investigación en Ingeniería de Aragón (I3A), Universidad de Zaragoza, 50018 Zaragoza, Spain.*

⁸*Departamento de Física, Universidad de Extremadura, 06071 Badajoz, Spain.*

⁹*Department of Physics, University of California, Santa Cruz, CA 95064, USA*

(Dated: September 16, 2021)

We perform numerical simulations, including parallel tempering, on the Potts glass model with binary random quenched couplings using the JANUS application-oriented computer. We find and characterize a glassy transition, estimating the location of the transition and the value of the critical exponents. We show that there is no ferromagnetic transition in a large temperature range around the glassy critical temperature. We also compare our results with those obtained recently on the “random permutation” Potts glass.

PACS numbers: 75.10Nr,64.60.Fr,05.10.Ln,75.40.Mg

I. INTRODUCTION

Potts models are among the building blocks of statistical mechanics, and their disordered versions (Potts glasses) are commonly used to describe a large class of anisotropic orientational glasses.¹ For example, if a crystal of molecular nitrogen is disordered by including some percentage of argon, the resulting compound, $\text{Ar}_{1-x}(\text{N}_2)_x$, is a disordered quadrupolar glass.² The Potts glass is one of the models of choice to describe materials of this type.

The four state ($p = 4$) pure Potts model in two dimensions ($D = 2$) describes the adsorption of N_2 on Kr in graphite layers.³ In $D = 3$ it describes the behavior of FCC antiferromagnetic materials (NdSb, NdAs and CeAs for example) where the magnetic field points in the $\langle 1,1,1 \rangle$ direction⁴. The site diluted version of the Potts model can describe, for example, the adsorption of hydrogen on the $(1,1,1)$ plane of nickel which has been previously disordered by inserting oxygen atoms.⁵ In this paper we will study the four state glassy Potts model, in which quenched random disorder induces frustration. This model presents at least three interesting theoretical problems that are still unsolved.

The *first* of these is the nature of the spin glass phase transition; one needs to reliably compute the critical temperature and the critical exponents in order to characterize the *universality class* of the model.

The *second* issue is how the qualitative features of phase diagram, including spin glass and ferromagnetic phases, evolve when going from the mean field models to realistic, finite dimensional models. For example, previ-

ous work^{6,7,8} has shown that, at low temperatures, the standard Potts glass (in which the Potts coupling between two spins can have positive or negative sign) develops spontaneous ferromagnetic ordering, which can affect, or even prevent, a spin glass phase transition. Furthermore, in mean field theory the value of this ferromagnetic transition temperature, T_{FM} , varies with the number p of Potts states as $T_{\text{FM}} = (p-2)/2$, which gives $T_{\text{FM}} = 1$ for the four state model. Mean field analysis also shows that for $p \leq 4$ the spin glass transition temperature (where replica symmetry gets broken) is $T_{\text{RSB}} = 1$: if $p = 4$ the two transition temperatures coincide. Hence an interesting open problem is to check whether or not this result, valid for $D = \infty$, also holds when the dimensionality is finite. Also relevant here is that, in the mean field picture, the $p = 4$ glassy model is “marginal”, since for $p \leq 4$ the transition is continuous whereas for $p > 4$ the order parameter $q(x)$ is discontinuous (even if, as usual in spin glasses, there is no latent heat).⁷ In a series of interesting papers Binder, Brangian and Kob⁹ (see also the recent work by Katzgraber, Lee and Young¹⁰) study the ten state glassy Potts model, and find that for such high number of states the mean field and the finite dimensional cases *are very different*. Here we investigate whether the same is true for $p = 4$.

The *third* relevant issue is again related to universality. In order to avoid a possible contamination of the spin glass transition point by the effects of the ferromagnetic phase, Marinari, Mossa and Parisi¹¹ have introduced a new class of glassy Potts models, the “random permutation” Potts glass, where a gauge symmetry protects the model against a ferromagnetic transition. This approach

has the advantage of being closer to reality since, in real quadrupolar glasses, ferromagnetism plays no role. One of these models has been thoroughly studied recently by some of the authors of the present work,¹² and its behavior found to be consistent with a Kosterlitz-Thouless phase transition. One of its signatures is that, below the critical point, data for the correlation length divided by lattice size, ξ/L , for different sizes merge into a single curve. However, given the precision of the numerical data and allowing for corrections to finite-size scaling, one cannot exclude a value of the lower critical behavior near and slightly below $D = 3$.

A further motivation for this study is to investigate how the behavior of the Potts glass changes with p . For $p = 3$, a Potts glass transition occurs¹⁰ with critical exponents $\nu \simeq 1.2$ and $\eta \simeq 0.02$, while, for $p = 10$, Ref. [9] finds no phase transition in agreement with Ref. [9]. In addition, we note the Ising spin glass model, which corresponds to $p = 2$, has $\nu \simeq 2.5$ and $\eta \simeq -0.4$ (see Ref. (13,14)). It would therefore be very interesting to get a consistent picture of how the nature of the Potts glass transition evolves with the number of states p .

In an attempt to give reliable answers to these questions, we have performed extensive numerical simulations using one unit of the JANUS dedicated computer (which has a total of 16 units).¹⁵ We have been able to thermalize the $p = 4$ Potts glass model on an $L = 16$ cubic lattice down to the low temperature phase: this gives us information on far larger lattice sizes than had been possible before.

The outline of the paper is the following. In section 2 we introduce our model and physical observables. In section 3 we describe the numerical methods that we have used in the simulations. In section 4 we describe our tests of thermalization and our approach to data analysis, and we analyze our findings, both for the overlap and for the magnetization. The main results are that we have been able to characterize the spin glass transition and that no onset of ferromagnetic order has been found at and below the spin glass transition point. We discuss these findings in section 5.

II. MODEL AND OBSERVABLES

In the p -state Potts model, each site i of a three dimensional cubic lattice of linear size L with periodic boundary conditions has a scalar spin s_i which takes one of the values $1, 2, \dots, p$. The Hamiltonian of the standard Potts glass model is

$$H = - \sum_{\langle i,j \rangle} J_{ij} \delta_{s_i, s_j}, \quad (1)$$

where the sum runs over all nearest neighboring sites. Two neighboring sites i and j interact with energy $-J_{ij}$ when their spin states s_i and s_j have the same value, and otherwise their energy is zero. The couplings J_{ij}

are independent quenched random variables taken from a bimodal distribution ($J_{ij} = \pm 1$) with zero average. From now on we will focus on the four-state ($p = 4$) case.

It is possible to represent the state of site i by a $(p-1)$ -dimensional vector, \mathbf{S}_i , equal to one of the p unit vectors \mathbf{S}_a pointing to the corners of a hyper-tetrahedron in $(p-1)$ -dimensional space. These vectors satisfy the relations

$$\mathbf{S}_a \cdot \mathbf{S}_b = \frac{p \delta_{ab} - 1}{p-1}. \quad (2)$$

Equation (2) defines the *simplex* representation, that we will use to describe the observables measured in the simulations.

In order to investigate the possible presence of (spurious) ferromagnetic effects we have carefully checked the value of the magnetization, looking for possible signs of spontaneous ferromagnetic ordering. In the simplex representation we define the vector magnetization as

$$\mathbf{m} = \frac{1}{N} \sum_{i=1}^N \mathbf{S}_i, \quad (3)$$

where $N \equiv L^3$ is the number of spins.

The existence of a possible transition to a ferromagnetic phase has been also analyzed by studying the magnetic susceptibility

$$\chi_M = N \overline{\langle |\mathbf{m}|^2 \rangle}, \quad (4)$$

where $\langle (\cdot \cdot \cdot) \rangle$ stands for the thermal average and $\overline{(\cdot \cdot \cdot)}$ denotes the disorder average.

To study the glass transition we define the spin-glass order parameter as a tensorial overlap between two replicas (i.e. two copies of the system defined with identical couplings whose spin values evolve independently). The standard definition of its Fourier transform with wave vector \mathbf{k} is¹⁰

$$q^{\mu\nu}(\mathbf{k}) = \frac{1}{N} \sum_i S_i^{(1)\mu} S_i^{(2)\nu} e^{i\mathbf{k} \cdot \mathbf{R}_i}, \quad (5)$$

where $S_i^{(1)\mu}$ is the μ -th component of the spin of the first replica in the simplex representation, and $S_i^{(2)\nu}$ is the ν -th component of the spin in the second replica.

The momentum-space, spin-glass susceptibility is defined by

$$\chi_q(\mathbf{k}) = N \sum_{\mu, \nu} \overline{\langle |q^{\mu\nu}(\mathbf{k})|^2 \rangle}. \quad (6)$$

We also define the correlation length ξ in terms of the Fourier transform¹⁶ in Eq. (6) as

$$\xi = \frac{1}{2 \sin(\mathbf{k}_m/2)} \left(\frac{\chi_q(0)}{\chi_q(\mathbf{k}_m)} - 1 \right)^{1/2}, \quad (7)$$

where \mathbf{k}_m is the minimum wave vector allowed within the lattice. Periodic boundary conditions imply that this

vector is $\mathbf{k}_m = (2\pi/L, 0, 0)$ or one of the two other related vectors in which the components are permuted. The definition in Eq. (7) arises naturally on a finite lattice.

We will base a large part of our analysis on the dimensionless correlation length ξ/L , i.e. on the correlation length divided by the lattice size. This quantity does not depend on L (asymptotically for large L) at the transition temperature, which allows us to obtain a precise estimate of T_c from the value of T at which data for different lattice sizes cross.¹⁶

III. NUMERICAL METHODS

We have simulated three dimensional cubic lattices with linear sizes $L = 4, 6, 8$ and 16 . Because spin-glass simulations have very long relaxation times, we used the parallel tempering (PT) algorithm¹⁷ to speed up the dynamical process that brings the system to thermal equilibrium and eventually explores it. Physical quantities are only measured after the system has been brought to equilibrium.

The dynamics is comprised of single-spin updates and temperature swaps. The single-spin updates are carried out with a sequential heat bath (HB) algorithm. We define a *Monte Carlo sweep* (MCS) as N sequential trial updates of the HB algorithm (i.e. every spin undergoes a trial update once).

The PT algorithm (applied to a given realization of the quenched disorder, that we will call a sample) is based on simulating a number of copies of the system with different values of the temperature but the same interactions. Exchanging the temperature of two copies with adjacent temperatures with a probability that respects the detailed balance condition is the crucial mechanism of PT. The result is that each copy of the system drifts in the whole allowed temperature range (that has been decided a priori). When a copy is at a high temperature it equilibrates fast and so each time it descends to low temperature it is likely to be in a different valley in the energy landscape.

The HB and the PT algorithms require high quality random numbers; we generate them with a 32-bit Parisi-Rapupano shift register¹⁸ pseudo-random number generator.

Details about our numerical simulations are summarized in Table I. The simulation of the smaller lattices, with $L = 4$ and 6 , was performed on standard computers. More powerful computational resources are needed to deal with the $L = 8$ and 16 systems, so we have studied them on a prototype board of the Janus¹⁵ computer, an FPGA based computer optimized for a relatively small set of hard computational problems (among them, spin glass simulations). A performance comparison between an Intel(R) Core2Duo(TM) processor and one Janus processor (one FPGA) shows that the latter is about one thousand times faster¹⁹ when simulating Potts models. JANUS has allowed us to thermalize a large number of

samples for bigger sizes than would have been feasible on a standard computer. The computational effort behind our analysis amounts to approximately 6 years CPU time on a 2.4 GHz Intel(R) Core2Duo(TM) processors for $L = 8$ and thousands of CPU-years for $L = 16$.

Data input and output is a critical issue for JANUS performance, so we had to carefully choose how often to read configuration data; in general, we end up taking fewer measurements than in simulations on a traditional PC. Having fewer (but less correlated) measurements does not affect the quality of our results. We read and analyze values of physical observables every 2×10^5 MCS for both $L = 8$ and 16 (see Table I for details).

L	N_{samples}	MCS	$[\beta_{\text{min}}, \beta_{\text{max}}]$	N_{β}	N_{HB}	N_m
4	1000	3.2×10^5	[2.0,6.0]	9	5	10^3
6	1000	8×10^5	[2.5,5.0]	7	5	10^3
8	1000	2×10^8	[2.7,4.2]	16	10	2×10^5
16	1000	8×10^9	[1.7,4.1]	32	10	2×10^5

TABLE I: For each lattice size we show the number of disorder samples that we have analyzed, the number of MCS per sample, the range of simulated inverse temperatures $\beta = 1/T$, the number of (uniformly distributed) β values used for PT, the number of MCS performed between two PT steps (N_{HB}), and the number of MCS between measurements (N_m).

On the larger lattices, we perform a PT step every 10 MCS while on the smaller lattices this value is 5. In a standard computer the PT algorithm takes a negligible amount of time, compared to a whole MCS. However, in JANUS the clock cycles needed by one PT step are more than those needed for a MCS. For this reason we chose to increase the number of MCS between two PT steps. However, this number should not be *too* large, as we do not want to negatively affect the PT efficiency. A preliminary analysis has been carried over to test how the PT parameter would affect the simulation results, and we have selected a value that seems to be well optimized (see Table I).

IV. RESULTS

A. Thermalization Tests

We start by briefly discussing the tests that we performed to check if our numerical data are really well thermalized. We use a standard test in which a given physical quantity is averaged (first over the thermal noise and then over the quenched disorder) over logarithmically increasing time windows. Equilibrium is reached when successive values converge. We emphasize that it is crucial for time to be plotted on logarithmic scale.

We are interested in the correlation length, defined in Eq. (7), which is plotted in Fig. 1 at the lowest simulated temperature (the hardest case for thermalization).

We see that the values of the correlation length reach a clear plateau for all sizes, strongly suggesting that our samples have reached thermal equilibrium. This analysis also provides useful information about the number of sweeps that have to be discarded at the beginning of the Monte-Carlo history in order to use only equilibrated configurations.

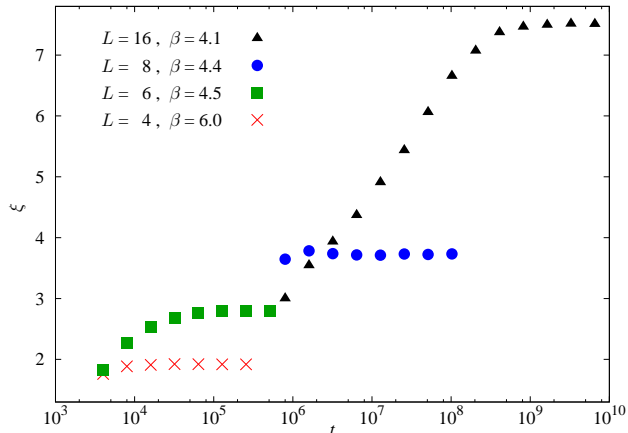


FIG. 1: A thermalization test. We show the behavior of the time dependent spin glass correlation length as a function of Monte Carlo time. We have averaged the correlation length using a logarithmic binning procedure. We show data for the lowest temperature simulated for each size.

B. Finite Size Scaling Analysis; The Quotient Method

To measure the critical exponents we used the quotient method.^{16,20} In this approach one compares results for lattice sizes L and sL for integer s which here we take to be 2. Firstly, for a pair of lattice sizes L and sL , we find the point, $\beta = \beta_{\text{cross}}$, where the correlation length divided by system size is equal for the two sizes, i.e.

$$\frac{\xi(sL, \beta_{\text{cross}})}{sL} = \frac{\xi(L, \beta_{\text{cross}})}{L}, \quad (8)$$

or equivalently

$$Q_{\xi}(L, sL) \equiv \frac{\xi(sL, \beta_{\text{cross}})}{\xi(L, \beta_{\text{cross}})} = s. \quad (9)$$

We then determine similar ratios for other observables. If an observable O diverges near the critical temperature as t^{-x_O} , where t is the reduced critical temperature, then we expect

$$Q_O(L, sL) \equiv \frac{O(sL, \beta_{\text{cross}})}{O(L, \beta_{\text{cross}})} = s^{x_O/\nu} + O(L^{-\omega}), \quad (10)$$

where ω is the exponent describing the leading corrections to scaling.

Applying Eq. (10) to the operators $\partial_{\beta}\xi$, and χ_q yields respectively the critical exponents $1 + 1/\nu$ and $2 - \eta_q$. Similarly, if we apply Eq. (10) to the magnetic susceptibility we obtain the exponent $2 - \eta_m$.

C. Overlap Critical Exponents

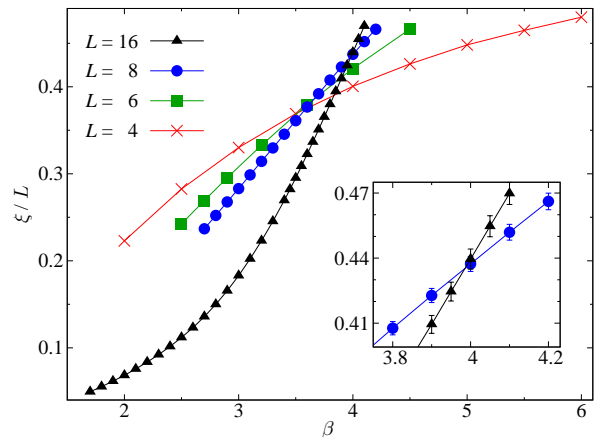


FIG. 2: The spin glass correlation length divided by L as a function of β for $L = 4, 6, 8$ and 16 . In the inset we magnify the crossing between the $L = 8$ and $L = 16$ curves.

In Fig. 2, we plot the correlation length (defined in Eq. (7)) divided by system size for different lattice sizes as a function of the temperature. According to Eq. (8), the data should cross if there is a transition. Indeed there are clear crossings, indicating a second order phase transition, though the values of β at which the crossings occur vary with system size. From Fig. 2 we determined the crossing values β_{cross} for the pairs of sizes (4, 8) and (8, 16), see Table II. By computing the spin glass susceptibility and the derivative of the correlation length at these crossing points, we obtain estimates of the corresponding effective critical exponents, η_q and ν , from Eq. (10) and also show these results in Table II. Since we have only data at a discrete set of temperatures, we needed an accurate interpolating procedure to determine the crossing points and the values of other measurables at these points. We chose to fit all available data with a cubic spline. To test that our results are independent of the interpolation procedure we also implemented a linear interpolation around the crossing point. We computed the crossing point and effective exponents with both procedures, and found agreement within the statistical precision of our results.

The two values of β_{cross} shown in Table II are rather different, suggesting large corrections to scaling, i.e. a small value for the correction exponent ω , so we do not have enough information to reliably compute asymptotic critical exponents. Nonetheless, from Table II we see that the trend of η_q with increasing size is very different

from what would be observed in the absence of a transition for which η_q would equal 2. Hence, our numerical data strongly support the existence of a spin glass phase transition at finite temperature.

(L_1, L_2)	$\beta_{\text{cross}}(L_1, L_2)$	$\nu(L_1, L_2)$	$\eta_q(L_1, L_2)$	$\eta_m(L_1, L_2)$
(4, 8)	3.59(4)	0.83(5)	0.15(4)	1.84(3)
(8, 16)	4.00(4)	0.96(8)	0.12(6)	2.06(3)

TABLE II: Results for the critical exponents using the quotient method. (L_1, L_2) are the two lattice sizes used and β_{cross} is the inverse temperature where the two curves of the dimensionless correlation length ξ/L cross (see Fig. 2). The values for ν and η_q are extracted from measurements involving the overlap q , whereas η_m has been computed from the magnetization. These results were obtained with the cubic spline interpolating procedure.

D. The Magnetization in the Critical Region

As discussed in the introduction, the standard Potts glass studied here could undergo a ferromagnetic phase transition at low T . This second transition could bias our analysis of the spin glass phase by influencing the behavior even close to the glass transition temperature (a serious problem if the two temperature values are very close). It is therefore important to investigate whether there is a region with non-zero spontaneous magnetization close to the spin glass critical region.

We have therefore computed, using the quotient method, the growth of the magnetic susceptibility, showing the results in the last column of Table II. The magnetic susceptibility diverges with an exponent $2 - \eta_m$, so $\eta_m \simeq 2$ is a clear footprint for the absence of a magnetic phase transition. For the two largest lattices we find a value statistically compatible with 2. Hence we can safely discard the scenario where a ferromagnetic transition appears at β_{cross} . We are observing just a glass transition.

In order to argue that there is no ferromagnetic transition in the *whole* temperature range studied, we computed the magnetization and susceptibility throughout this range. In the paramagnetic phase, the magnetization is random in sign so its modulus $\langle |\mathbf{m}| \rangle$ is proportional to $1/\sqrt{N}$, and the magnetic susceptibility $\chi_M = N \langle |\mathbf{m}|^2 \rangle$ is independent of size. By contrast, in a ferromagnetic phase, $\langle |\mathbf{m}| \rangle$ tends to a positive value at large N so χ_M diverges proportionally to N .

In the main part of Fig. 3 we plot χ_M versus the inverse of the temperature. In the glass pseudo-critical region, $\beta \sim 3.5 - 4$, the two largest lattices give very similar results, so we recover the result $\eta_m=2$ quoted in Table II. Furthermore, at *no* temperature does the susceptibility increase strongly with size. Similarly, the magnetization, shown in the inset of Fig 3, decreases rapidly with size, which also indicates paramagnetic behavior.

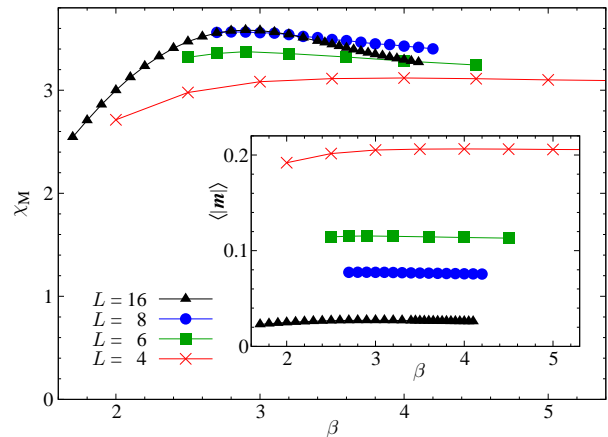


FIG. 3: We show the behavior of the magnetic susceptibility, χ_M , versus the inverse temperature. Notice that this susceptibility saturates in the critical region. In the inset we have plotted the average of the modulus of the magnetization, $\langle |\mathbf{m}| \rangle$, against the temperature: this observable behaves as $1/\sqrt{N}$ which clearly signals a paramagnetic behavior.

From Fig. 3 we conclude that there is no ferromagnetic phase in the region $\beta \in [0, \simeq 4.5]$.

V. CONCLUSIONS

In this study we have numerically explored the equilibrium behavior of a Potts glass with binary couplings on large lattices ($L \leq 16$). A prototype board (16 FPGA processors) of the Janus¹⁵ optimized computer, using a parallel tempering algorithm¹⁷, has allowed us to do this for the first time.

By computing the critical exponent associated with the magnetic susceptibility, and by analyzing the behavior of the magnetization in the critical region, we have shown that a paramagnetic-ferromagnetic phase transition does not occur. This result is different from mean field theory where, for general p , one sees both ferromagnetic and spin glass transitions at temperatures which become equal for $p = 4$.

We have found and characterized a spin-glass phase transition with critical exponents $\nu \simeq 1$, $\eta_q \simeq 0.1$ and hence $\beta_q \simeq 1/2$. In order to extrapolate these values to the thermodynamic limit, larger lattice sizes need to be simulated (which we will try to accomplish in the near future). The critical exponents computed here are compatible with known values for other values of p . We note that the exponent ν decreases with increasing number of states p , since $\nu = 2.45(15)$ for $p = 2$ (see Ref. [13]) and $\nu = 1.18(5)$ for $p = 3$ (see Ref. [10]). The values presented in Table II for $p = 4$ are consistent with this decrease which is expected to end when $\nu = \tilde{\nu} = 2/D = (= 2/3$ in $D = 3)$, since a finite size scaling estimate implies that, for a disordered system, the transition is then first order.²² Similarly, the expo-

nent η grows with p since $\eta = -0.375(10)$ for $p = 2$ and $\eta = 0.02(2)$ for $p = 3$, while our estimates in Table II are larger.

The hypothesis of a disordered first order phase transition provides an upper bound $\eta = 1/2$ (since the susceptibility is expected to grow as $L^{d/2}$). In the mean field solution of Potts glass, second order phase transitions are found for small values ($p \leq 4$), but a first order transition is found⁷ for $p > 4$. An interesting problem for future study is whether the transition remains second order at large p for short-range spin glasses in three dimensions or whether, for a given value of $p > 4$, the second order transition disappears (in a tricritical point) to be replaced by a first order phase transition at larger p .²⁴

We have studied the standard Potts glass which is expected to be in the same universality class as the permutation Potts glass¹¹. However, the the present state of the art in numerical simulation does not enable us to confirm this. In the permutation Potts glass one does not observe a clear cut phase transition. Instead of a crossing point there is a smooth merging of the curves for different lattice size. This could indicate transient behavior, i.e. there is really a phase transition but it is only visible on larger lattices, or a Kosterlitz-Thouless like transition.¹² For the standard Potts glass studied

here, we find a finite transition as indicated by a crossing of the correlation length data in Fig. 2. However, we note that the crossing point shifts to larger β , i.e. smaller T , at larger sizes. It is therefore possible that asymptotic critical behavior could be quite marginal, as is found in the permutation Potts glass. Consequently the standard and permutation Potts glass models *may* be in the same universality class, but larger sizes are needed to confirm this.

Acknowledgments

Janus has been funded by European Union (FEDER) funds, Diputación General de Aragón (Spain), Microsoft–Italy and Eurotech. We were partially supported by MEC (Spain) through contracts TEC2007-64188, FIS2006-08533, FIS2007-60977 and FIS2008-01323, from CAM (Spain) under contract CCG07-UCM/ESP-2532, and from the Microsoft Prize 2007. D. Sciretti acknowledges an FPI fellowship BFM2003-08532-C03-01 from MEC (Spain). The authors would like to thank the Arénaire team, especially Jérémie Detrey and Florent de Dinechin for the VHDL code of the logarithm function.²³

-
- ¹ K. Binder and J. D. Reger, *Adv. Phys.* **41**, 547 (1992); K. Binder, *Quadrupolar Spin Glasses*, in *Spin Glasses and Random Fields*, edited by A. P. Young (World Scientific, Singapore 1997); K. Binder and W. Kob, *Glassy Materials and Disordered Solids* (World Scientific, Singapore 2005).
- ² U. T. Höchli, K. Knorr and A. Loidl, *Adv. Phys.* **39**, 405 (1990).
- ³ E. Domany, M. Schick y J. S. Walker, *Phys. Rev. Lett.* **38**, 1148 (1977).
- ⁴ E. Domany, Y. Shnidman y D. Mukamel, *J. Phys. C* **15** L495 (1982).
- ⁵ L. Schwenger, K. Budde, C. Voges y H. Pfnür, *Phys. Rev. Lett.* **73**, 296 (1994); *Phys. Rev. B* **52**, 9275 (1995).
- ⁶ D. Elderfield and D. Sherrington, *J. Phys. C* **16**, L971 (1983).
- ⁷ D. J. Gross, I. Kanter and H. Sompolinsky, *Phys. Rev. Lett.* **55**, 304 (1985).
- ⁸ E. De Santis, G. Parisi and F. Ritort, *J. Phys. A* **28**, 3025 (1995).
- ⁹ C. Brangian, W. Kob and K. Binder, *Europhys. Lett.* **53**, 756-761 (2001), arXiv:cond-mat/0009475; *Phil. Mag. B* **82**, 663 (2002), arXiv:cond-mat/0104355; *J. Phys. A : Math. Gen.* **35**, 191 (2002), arXiv:cond-mat/0106314; *Europhys. Lett.* **59**, 546 (2002), arXiv:cond-mat/0202232; *J. Phys. A: Math. Gen.* **36**, (2003) 10847, arXiv:cond-mat/0211195.
- ¹⁰ L. W. Lee, H. G. Katzgraber and A. P. Young, *Phys Rev. B* **74**, 104416 (2006), arXiv:cond-mat/0605010.
- ¹¹ E. Marinari, S. Mossa and G. Parisi, *Phys. Rev. B* **59** 8401 (1999).
- ¹² L. A. Fernández, A. Maiorano, E. Marinari, V. Martin-Mayor, D. Navarro, D. Sciretti, A. Tarancón, J. L. Velasco, *Phys. Rev. B* **77**, 104432 (2008).
- ¹³ M. Hasenbusch, A. Pelissetto and E. Vicari, *J. Stat. Mech.* L02001 (2008). M. Hasenbusch, A. Pelissetto and E. Vicari, arXiv:0809.3329
- ¹⁴ H. G. Katzgraber, M. Körner and A. P. Young, *Phys. Rev. B*, **73**, 224432 (2006).
- ¹⁵ F. Belletti, M. Cotallo, A. Cruz, L. A. Fernández, A. Gordillo, A. Maiorano, F. Mantovani, E. Marinari, V. Martin-Mayor, A. Muñoz-Sudupe, D. Navarro, S. Perez-Gaviro, J. J. Ruiz-Lorenzo, S. F. Schifano, D. Sciretti, A. Tarancón, R. Tripicciono, J. L. Velasco *et al.*, *Simulating spin systems on IANUS, an FPGA-based computer*, *Comp. Phys. Comm.* **178**, 3, 208 (2008)
- ¹⁶ See, e.g., D. J. Amit and V. Martin-Mayor, *Field Theory, the Renormalization Group and Critical Phenomena*, (World-Scientific Singapore, third edition, 2005).
- ¹⁷ M. Tesi, E. Janse van Resburg, E. Orlandini and S. G. Whittington, *J. Stat. Phys.* **82**, 155 (1996); K. Hukushima and K. Nemoto, *J. Phys. Soc. Jpn.* **65**, 1604 (1996); E. Marinari, *Optimized Monte Carlo Methods*, in *Advances in Computer Simulation*, edited by J. Kertész and Imre Kondor (Springer-Verlag, Berlin 1998), p. 50, cond-mat/9612010; E. Marinari, G. Parisi and J. J. Ruiz-Lorenzo, *Numerical Simulations of Spin Glass Systems in Spin Glasses and Random Fields*, edited by A. P. Young (World Scientific, Singapore, 1997).
- ¹⁸ G. Parisi and F. Rapuano, *Phys. Lett. B* **157**, 301 (1985).
- ¹⁹ F. Belletti, M. Cotallo, A. Cruz, L. A. Fernández, A. Gordillo, A. Maiorano, F. Mantovani, E. Marinari, V. Martin-Mayor, A. Muñoz-Sudupe, D. Navarro, S. Perez-Gaviro, J. J. Ruiz-Lorenzo, S. F. Schifano, D. Sciretti, A.

Tarancón, R. Tripiccion, J. L. Velasco *et al.*, *JANUS: an FPGA-based System for High Performance Scientific Computing*, to be published in *Computing in Science & Engineering*

- ²⁰ H. G. Ballesteros, L. A. Fernández, V. Martín-Mayor and A. Muñoz Sudupe. Phys. Lett. **B378**, 207 (1996).
- ²¹ G. Parisi, *Statistical Field Theory*, (Addison Wesley, 1998).
- ²² A. Maiorano, V. Martin-Mayor, J.J. Ruiz-Lorenzo and A. Tarancon, Phys. Rev. B **76**, 064435 (2007).
- ²³ J. Detrey and F. de Dinechin. "Parameterized floating-point logarithm and exponential functions for FPGAs". Special Issue on FPGA-based Reconfigurable Comput-

ing, Microprocessors and Microsystems **3**, **31(8)**, 537-545 (2007).

- ²⁴ Notice that the inverse critical temperatures for the p -state Potts glass model follow well the law: $\beta_c(p) \simeq p$ (e.g. $\beta_c(p = 2) \simeq 2 \times 0.90 = 1.80$; $\beta_c(p = 3) \simeq 2.65$ and in this work $\beta_c(p = 4) \simeq 4$). If this empirical law is accurate, we would expect $\beta_c(p = 10) \simeq 10$. This appears to contradict the conclusions of Refs. [9,10], who argued that there is no transition for $p = 10$. However, we note that virtually all the data in those papers is for values of β smaller than 10.